CANADA

DEPARTMENT OF
ENERGY, MINES AND RESOURCES
MINES BRANCH
OTTAWA

DYNAMIC TOUGHNESS - ITS RELEVANCE AND MEASUREMENT

L. P. TRUDEAU

PHYSICAL METALLURGY DIVISION

OCTOBER 1974

Research Report R 275

Price: .50 cents

Available by mail from Information Canada, Ottawa, K1A 0S9
and at the following Information Canada bookshops:

HALIFAX
1683 Barrington Street

MONTREAL
640 St. Catherine Street West

OTTAWA
171 Slater Street

TORONTO
221 Yonge Street

WINNIPEG
393 Portage Avenue

VANCOUVER
800 Granville Street

or through your bookseller

Price: .50 cents Catalogue No. M38-1/275

Price subject to change without notice

Information Canada
Ottawa, 1974

Mines Branch Research Report R 275

DYNAMIC TOUGHNESS - ITS RELEVANCE AND MEASUREMENT

by

L. P. Trudeau*

ABSTRACT

A 1967 Research Report (R 190) showed how dynamic or crack propagation toughness could be the governing quantity for failure under quasi-static loads. Tensile tests done as a check on the theory established some bounds on the dynamic toughness of a steel plate. This plate was used as a "calibration standard" in the development of a test to measure dynamic toughness directly. The test development is apparently successful using an instrumented dynamic bend specimen 17 in. (430 mm) long, 1 1/2 in. (38 mm) deep and 1/4 to 2 in. (6 to 51 mm) thick, with a crack one half the depth, and broken on a 10 in. (254 mm) span with a drop height of 17 in. (430 mm). The load is measured on the tension side with a strain gauge 2.0 in. (51 mm) from the crack. Load rise time varies with the toughness but for low toughnesses is about 0.1 millisec. Test results for four steels (CSA G40.4, 40.11B, 40.12B and 40.18) over the temperature range from -75°C to room temperature are given. The applicability of the data are discussed.

---

*Research Scientist, Engineering Physics and Refractory Metals Section, Physical Metallurgy Division, Mines Branch, Department of Energy, Mines and Resources, Ottawa, Canada.

Direction des Mines
Rapport de recherche R 275

TENACITE DYNAMIQUE: SON APPLICABILITE ET SES MESURES

par
L. P. Trudeau*

RESUME

Dans un rapport de recherche de 1967 (R 190), on a démontré comment la ténacité dynamique ou la ténacité à la propagation d'une fissure pouvait être le facteur prédominant d'une fissure sous des charges quasi-statiques. Dans le but de vérifier cette théorie, on a effectué des essais de tension afin d'établir la ténacité dynamique limite d'une plaque d'acier. Cette plaque a été utilisée comme étalon dans l'élaboration d'un essai direct de la ténacité dynamique. L'élaboration de l'essai est apparemment un succès lorsqu'on utilise un échantillon de pliage dynamique instrumenté de 17 po. (430mm) de long, de 1½ po. (38mm) de profond et de ¼ à 2 po. (6 à 51mm) d'épais, avec une fissure longue de la moitié de la profondeur et cassée sur un écartement de 10 po. (254mm), avec une hauteur de chute de 17 po. (430mm). La charge est mesurée du côté de la tension avec une jauge de déformation à 2 po. (51mm) de la fissure. Le temps de montée de la charge varie selon la ténacité, mais le temps pour de faibles ténacités est de 0.1 millisec. On a donné les résultats d'essais de quatre aciers (CSA G40.4, 40.11B, 40.12B et 40.18) sur une échelle de température allant de -75°C jusqu'à la température de la pièce. L'applicabilité des données y est discutée.

---

*Chercheur scientifique, Section de la physique appliquée et des métaux refractaires, Division de la Métallurgie physique, Direction des Mines, Ministère de l'Energie, des Mines et des Ressources, Ottawa, Canada.

CONTENTS

1. INTRODUCTION

The suitability of lower-strength ferritic steels for some applications, especially at comparatively low-ambient temperatures, is now assessed by empirical correlation tests, of which the one in widest use is the Charpy V-notch impact test. The common characteristic of these empirical tests for rating the tendency to brittle fracture, at least in so far as current specifications are concerned, is that they involve impact, i.e., dynamic loading.

Work at this laboratory over the past several years has been motivated by a desire to reduce the empiricism by substituting more direct and potentially quantitative physical concepts. An outline of our views seems to be a necessary preliminary for an appreciation of the reasons for the choices made in the quantitative dynamic test development to be described.

2. BACKGROUND THEORY

The size scale of tests for the properties of interest was set by the consideration that most of the applications encountered involve plate thicknesses of less than 2 in. (51 mm) and the credible sizes of defects are small, usually less than 1 in. (25 mm). In a typical instance, the specification calls for a minimum Charpy V energy at some minimum service temperature and the question arises as to what this energy means in relation to dynamic toughness and how this toughness may vary over a plate thickness range from 1/4 in. to 2 in. (6 to 51 mm) in the structure.

Service failures usually occur under quasi-static loads and numerous slow strain-rate tests of these materials with cracks in them have been reported but low-stress failures were not obtained at the failure temperature. That is, on the average, the

cracked strength is adequate. Pre-cracked tension tests are easiest to interpret in terms of strength and the results are shown schematically by the solid line in Fig. 1. Then, in the further investigation of the failure, a Charpy V-notch impact test curve is determined as shown dotted in Fig. 1. It is found that the failure correlates with a low impact energy. The loading rates in the tension test and the impact test are enormously different with a commonly quoted ratio of rates being 10^6. In References 1 and 2 it was suggested that a dynamic test correlated with the static failure because an increment of fracture introduced local dynamic loading. The local ductility at the defect was, for some reason, low - much lower than the average developed by the material. Mechanical or metallurgical damage can impair the local ductility.

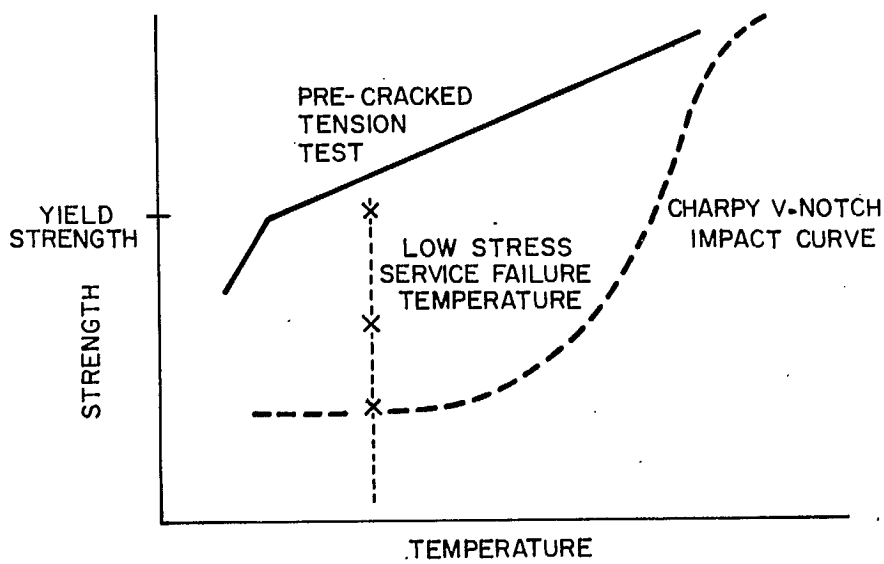

Fig. 1. Schematic illustration of strengths under static and impact loading. The strengths are different because at high strain rates the yield strength is increased by a factor of 2 to 3 or more. The higher yield strength increases the tensile stresses in the crack-tip region thus promoting crystallographic cleavage or reduced ductility and the higher strength also preserves constraint to much higher nominal stresses.

To check this, a series of slow strain-rate tension tests was reported in Reference 2 in which the local ductility at the base of a 1/2-in. (12 mm) deep-edge notch in 3/4-in. (19 mm) thick plate samples 4 in. (100 mm) wide was impaired by local nitriding or electron beam welding. The local ductility was impaired over as small a distance as possible and the indications were that this distance was not more than a few thousandths of an inch with low residual stresses. When these specimens were tension tested, fractures occurred at various strength levels, as shown by the x's in Fig. 1, with the strength being dependent on the combination of notch root radius and ductility which determined when the fracture started. If a number of such tests are done then one can expect eventually, by chance, to determine a low upper bound on the dynamic toughness or to bracket this toughness by two specimens which, within narrow stress limits will show, in one case, failure and in the other an arrested short fracture.

For the tension tests reported in Reference 2 an upper bound of 21 ksi$\sqrt{\text{in}}$. (23 MPa$\sqrt{\text{m}}$) at -67°C was found for one plate. This failure occurred at an average stress on the net section of 16.4 ksi (113 MPa) whereas specimens fatigue-cracked to a somewhat deeper notch broke at net stresses close to 40 ksi (276 MPa) at the same temperature. On this same plate an arrested fracture at 39.6 ksi (272 MPa) at -35°C, and a failure at 41.3 ksi (285 MPa) at -15°C allow some additional assessment of dynamic toughness.

This technique allows dynamic toughness determination under a realistic simulation of one class of service failure. Because most specimens will not start cracking close to the limiting propagation condition, most specimens are, in effect, wasted. A technique for the direct determination of the same quantity is desired so this plate was used as a "calibration standard" in the dynamic test development. While it is considered most likely that this definite minimum dynamic toughness exists, understanding of its role in a service failure can be complicated, first by inertial effects associated with initiation, second by

the vibration characteristics of the structure and third, and most important, by the general implications of ductility.

In connection with inertial effects associated with initiation, it may be noted that, in these tension tests, the brittle layer was orders of magnitude smaller than the 1/2-in. (12 mm) notch. The sudden release of local stress by cracking of the brittle layer probably exerted little influence on the stress intensity calculated from the nominal stress and the notch geometry. At the other extreme, one may have an extensive brittle region resulting from locally applied heat or heavy mechanical damage and the sudden fast fracture of this layer may constitute the originating fast fracture. In this case, the sudden release of load over the full damage depth would be expected to cause the crack faces to open beyond the static equilibrium value and, in the limit, the applied stress intensity could be twice as high, momentarily, as that calculated from the nominal stress and the damage zone depth. There is some discussion of this in the Appendix of Reference 2. This vibration of the crack faces can be important and in a similar, related way, the vibration characteristics of the structure can play a major role in crack propagation or arrest by causing the stress on the material to fluctuate from values in excess of the nominal to values below it.

A major limitation in the choice of a quantitative dynamic test type and in the application of K_{Id} dynamic toughness values arises from the effects of ductility. The stress intensity parameter is derived from infinitesimal elasticity theory so the strains and displacements involved in the fracture have been assumed to be small. Finite stretching or distortion that is necessary to exhaust ductility as fracture progresses is not accounted for at all in the stress intensity. If the material has appreciable propagation ductility, the applicability of K_{Ic} or K_{Id} to the calculation of a failure condition depends on whether the load in the structure can follow the finite distortion at the requisite speed. In a rigid structure that is not free to distort,

very little ductility can be adequate to prevent the occurrence of more than an arrested "pop-in" increment of crack growth. In the case of a cracked part under constant load in bending or one containing pressurized fluid, a high ductility may not prevent failure if the necessary distortion can occur.

When the K parameter is associated with a strain-energy-release rate, G, as is usually the case, the ductility or displacement limitations can be recognized from physical considerations. The mechanism of strain-energy release is an elastic unloading wave so this type of analysis only gives a sufficient condition for failure if the displacement requirements can be supplied by an elastic unloading wave as the fracture propagates.

One can infer the general trend from tension tests such as those reported in Reference 2. The edge notch was 1/2 in. (12 mm) in a specimen width of 4 in. (100 mm) and wedge grips inhibited rotation of the halves of the 22 in. (560 mm) long specimens so the load was primarily tension with a comparatively small bending component. Fast fracture speeds up to 7500 fps (2280 mps) have been measured[3], so if we assume a speed of about 5000 fps (1500 mps) this is close to one third of the fastest elastic wave propagation velocity. When, for example, the fracture has travelled 1 in. (25 mm), the maximum travel distance of the elastic unloading wave is about 3 in. (76 mm) so the contraction resulting from this unloading is the only displacement available to exhaust the ductility. In the specimen mentioned earlier, the net stress was 16.4 ksi (113 MPa) and the nominal stress 14.2 ksi (98 MPa) so this displacement is small. The material must have nil dynamic ductility and this accords with the fracture appearance. Near the empirical drop-weight nil ductility temperature (ASTM E 208) it was found, for this low-strength steel, that the starting increments of fracture had to occur above the slow strain-rate yield stress on the net section for complete failure to occur. Such a fracture has oblique lips about 1/16 in. (1.6 mm) wide at the surfaces. This fracture would be expected

to run with a lower velocity because the elastic unloading wave would probably travel further to develop the necessary displacement and because the plastic flow process necessary for fracture would take more time. At higher temperatures where the propagation ductility increases further, one would expect to reach a condition where elastic unloading in a structure of ordinary size would be insufficient to supply the displacement required and the necessary movement and work has to come from a fast response load. An example of this is a mechanically damaged pipe which has both a hardened surface layer as well as denting and the pressurized gas acts as a fast response load to cause finite displacements as the layer cracks and the dent tends to "iron out".

There are, then, two aspects of fracture to be taken into account; one a stress intensity or force requirement must be satisfied if failure is to occur and, two, a movement or kinematic requirement for exhausting propagation ductility must also be met. The K_{Ic} or K_{Id} parameter is a measure of the minimum force needed but does not take the implications of propagation ductility into account. On the other hand, the drop-weight nil ductility test is a purely kinematic sorting test in which no forces are measured. The test is useful because it determines the temperature below which a small bend angle gives enough movement to accommodate a propagating fracture.

Reflection on what is being measured by the K_I parameter indicates that it is the constrained ductility at the crack tip and this is supported by measurement[4,5]. The inference from measurements on steels of different strength levels was that the tip strain was determined by the general level of the elastic strain field up to the point of general collapse of thickness constraint. Loss of constraint in this sense is at a far higher K level than the limit for a valid plane strain test by ASTM E 399. While the relationship of tip strain to K appears to be constant up to this point, the cracking tendency is not constant because surface profile studies suggest that the thickness or Z direction stress is decreasing long before this point.

Vosikovsky's measurements indicate that the linear strain, ε_y, at the tip is proportional to $K^{1.85}$ while the quadratic or tensorial strain, which in this principal strain case is $\gamma_{yy} = \varepsilon_y + 1/2\ \varepsilon_y^2$, is accurately proportional to K^2. Considering K as a quantity related to tip strain rather than to elastic strain energy release avoids the physical limitation inherent in the latter.

High K values involve strains well up into the finite range and are accompanied by noticeable distortion in specimens of ordinary size. If this distortion is supplied both in the structural application by a fast response load and in a specimen that simulates the application, then there seems to be a possibility for a quantitative treatment of higher ductility dynamic toughness in such structures. As always, though, the nominal stress must be added to the K parameter for a more complete solution and the relative importance of the role of the nominal stress sets a limit on the usefulness of just considering K.

3. TEST DEVELOPMENT

In order to minimize kinematic complications in the measurement of K, the first consideration in the choice of a test was to be able to supply, at the rate required, any movement necessary to exhaust ductility. For simplicity in loading, this leads to a bend specimen loaded by a heavy falling weight or a heavy pendulum. A heavy weight (the heavier the better) is mentioned because the weight should follow through with a constant velocity during fracture with little tendency to slow down or bounce. To reduce inertial effects, the minimum impact velocity consistent with the measurement of crack propagation toughness is desirable and a heavy weight is also helpful in this regard because of its higher energy.

Previous dynamic tests with these characteristics were those reported by Shoemaker and Rolfe[6]. They used instrumentation on their 1-in. (25 mm) thick specimens rather than on the striking tup and this practice we have also followed. Beyond these general similarities, our requirements have led us to change most of the parameters and each of these changes has necessitated some development work. A crack depth of one half the specimen depth has been adopted for all tests in order that the geometry factor table in ASTM E 399 could be used.

After the foil strain gauges (which had a 1/8-in. (3.2 mm) gauge length) had been applied, a calibration of load versus gauge output was done in a tensile machine. Then, accepting that the elastic modulus is practically independent of strain rate and temperature over the temperature range of interest, the maximum load can be obtained from the oscillograph trace of the dynamic test. This load and the specimen geometry are all that are needed for a calculation of the dynamic toughness. A soft aluminum damping pad about 1/16 in. (1.6 mm) thick was placed on the load impact location but it is questionable if this is necessary. A photograph of the apparatus is given in Fig. 2.

It has been mentioned that it was desired to test specimens over the thickness range 1/4 to 2 in. (6 to 51 mm). The usual practice in K_{Ic} testing is to have the specimen size proportional to the thickness. Because of the effects of vibration in dynamic testing, this approach was not considered suitable. The fundamental vibration period of a specimen is proportional to the square of its length, inversely proportional to depth and independent of thickness. The smaller specimens would have a period much shorter than the load rise time and consequently a smooth load rise would not be obtainable in the specimen. In order to decrease ambiguity in the interpretation of the oscillograph traces, it was decided to maximize the vibration period and to have it constant for all tests.

Early trials were with a specimen 24 in. (610 mm) long and 1 1/2 in. (38 mm) deep with a fundamental frequency of about 500 cps or Hz, but this specimen proved to be too long to be compatible with all requirements. Tested on a 16-in. (406 mm) span with drop heights up to 17 in. (430 mm) with a 1300-lb (590 kg) weight, smooth stress traces were not obtained and the maximum load on specimens from the "calibration plate" was about 50% too high. Various explanations are possible, but it was thought that the impact velocity might be too low to prevent a stop-start action of the fracture. Decreasing the span length to 10 in. (254 mm) to increase the rotational velocity of the specimen halves led to smooth traces, but excessive specimen overhang beyond the span supports caused an inertial effect, resulting in displacement of the stress traces away from the zero stress line. Decreasing the specimen length to 17 in. (430 mm), which resulted in doubling the fundamental frequency to 1 kHz, eliminated this stress trace displacement. The 17-in. (430 mm) specimen length has been used for all subsequent tests. For the 2-in. (51 mm) thick specimens the thickness is greater than the depth but this has been found to be acceptable because of the shape of the shear stress lobes[5].

The stress distribution in the specimen and the influence of strain gauge position on the apparent toughness were then investigated. The outputs of two strain gauges were monitored by the two channels of the oscilloscope and the time of cracking was indicated by brightening pulses from narrow foil strips cemented across the fracture path. At a location 2 in. (51 mm) from the crack, gauges on the tension and compression sides showed that the stress distribution was close to a static one but the stress on the compression side was always higher (see Fig. 3). It is suspected that this is caused by the loading weight accelerating under gravity rather than having a uniform velocity. While there was an approximately static-type stress distribution at this location, the moment distribution along the beam was far from linear (see Fig. 4 where the stress 3 1/2 in. (89 mm) from the crack was close to zero when the specimen started

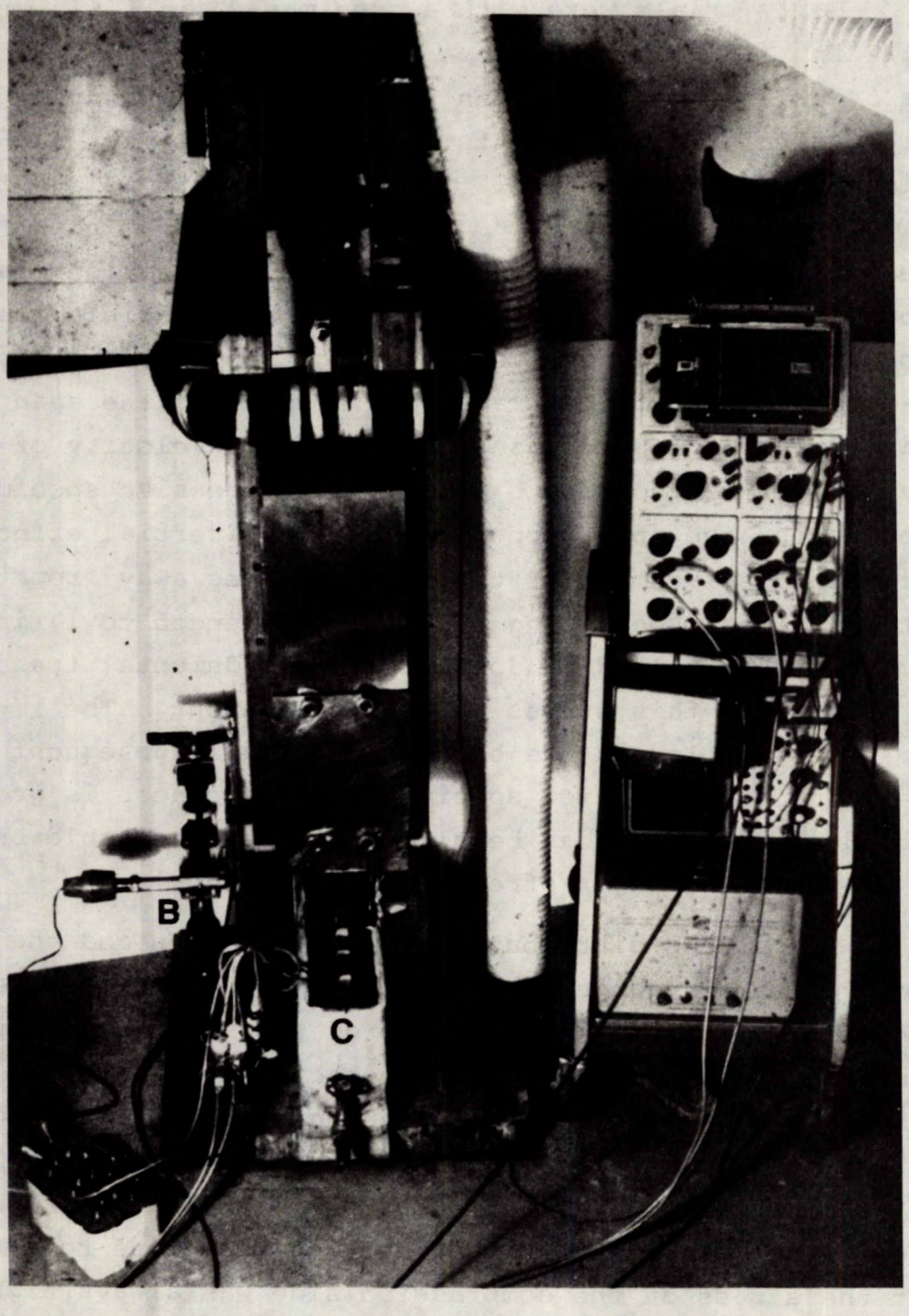

Fig. 2. Test apparatus with a weight of approximately 1300 lb (590 kg) at A, photocell trigger at B and cooling tank (C) in which the specimen sits on a bend fixture. The photocell trigger is to activate the 2-channel oscilloscope at right.

to break). Because the stress distribution is a pulse proceeding down the bar, the placement of the strain gauge used to monitor the load is important. It has been found that the strain gauge should be located so that the load peak coincides with the time of fracture. As an incidental point, it may be noted in these pictures that the tension side gauge, for instance, shows a compression dip before the build-up of tension. Measurements on the position of this compressive peak as a function of gauge location on the bar indicated that it was caused by the initial compressive pulse from the impacting weight showing up on the tension side before being reflected back as a tension pulse.

A gauge position at least 2 in. (51 mm) from the crack was preferred because this was about 3 times the crack length and, from St. Venant's Rule, the influence of the crack on the stress distribution should be small. Actually, a gauge position 2.0 in. (51 mm) from the crack on the tension side, a 10-in. (254 mm) span and a drop height of 17 in. (430 mm) were found to be the optimum conditions and were used for all of the data points. Under these conditions the load peak coincides with the time of fracture. As an illustration of the variation that can be caused by test variables, some tests can be cited in which the parameters were the same as given except that the span was decreased to 8 in. (203 mm). The load peak occurred before the specimen broke and was only one half as high so the apparent toughness was changed by a factor of 2.

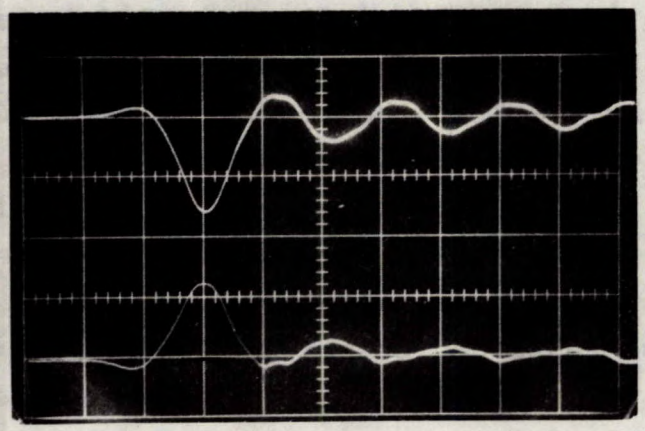

Fig. 3. Stress traces for G40.8 steel 2 in. (51 mm) thick tested at -73°C with a horizontal time scale of 0.2 millisec per major grid line and a vertical scale of 200 microstrain per major grid line. The gauges were 2 in. (51 mm) from the crack with the tension side trace at the bottom and the compression side at the top. The dynamic toughness was 25 ksi$\sqrt{\text{in.}}$ (27 MPa$\sqrt{\text{m}}$), and note that the specimen broke during the initial stress peak because the stress subsequently oscillates about the zero line. During the prior low-strain-rate calibration of the specimen the strains on the tension and compression sides were equal.

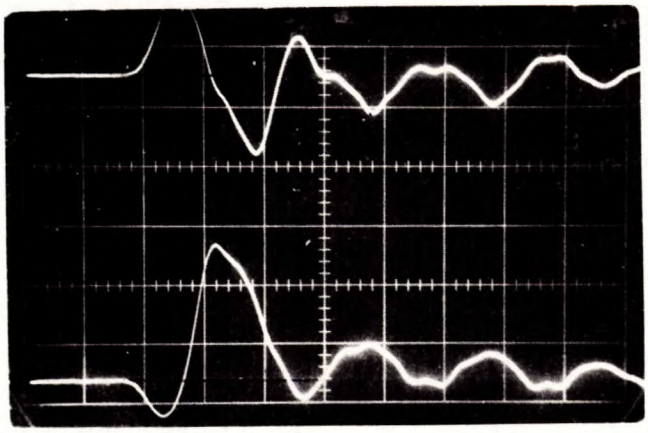

Fig. 4. Stress traces for G40.4 steel 1 in. (25 mm) thick tested at -39°C with a horizontal time scale of 0.2 millisec per division and a vertical scale of 100 microstrain per division. Both gauges were on the tension side with the lower at the regular measurement position 2 in. (51 mm) from the crack and the upper 3 1/2 in. (89 mm) from the crack. The span length was 10 in. (254 mm) so the latter gauge was 1 1/2 in. (38 mm) inside the span support. At the time the specimen broke, as shown by the peak on the lower trace, the stress at the other gauge was close to zero. The lower trace shows tension up, and the upper shows tension increasing in the downward direction. The dynamic toughness was 23 ksi$\sqrt{\text{in}}$. (25 MPa$\sqrt{\text{m}}$) and, again, the stress oscillates about zero after the initial peak so the specimen broke completely during the initial stress excursion.

Using the "calibration plate" for which one tension test at -67°C had given K_{Id} = 21 ksi$\sqrt{\text{in}}$. (23 MPa$\sqrt{\text{m}}$) and with the optimized test conditions, dynamic tests at -65 to -73°C have given values of 23.3, 28.0 and 21.8 ksi$\sqrt{\text{in}}$. (25.6, 30.8 and 24.0 MPa$\sqrt{\text{m}}$). This has lead to some confidence that the relevant quantity is being measured. The dynamic test values are slightly higher and the probable cause for this lies in the fatigue pre-cracking. A high-frequency Avery pulsator machine was used and the combined cyclic load plus holding load resulted in an applied stress intensity of about 27 ksi$\sqrt{\text{in}}$. (30 MPa$\sqrt{\text{m}}$). The

cyclic component was about 0.6 of the total and several hundred thousand cycles were used to grow a crack from the 1/2-in. (12.7 mm) machined notch depth to the final 3/4-in. (19 mm) depth. Of course, the maximum applied stress intensity during pre-cracking should be below the fracture stress intensity, if possible, because residual stress may affect the result.

4. RESULTS

Dynamic test results for 4 steels (CSA G40.4, 40.11B, 40.12B and 40.18) over the thickness range 1/2 in. to 2 in. (12 to 51 mm), with some for 1/4 in. (6 mm) thickness, and over the temperature range from -75°C to room temperature are given in Fig. 5 to 8. The thinner specimens were machined from the 2-in. (51 mm) thick plate. All specimens were longitudinal, that is with their length along the rolling direction and the notch or crack perpendicular to the plate surface. Charpy specimens were taken from 1/4 and mid-thickness locations in all plates. Except for the quenched and tempered plate data shown in Fig. 8, the differences in Charpy properties through the plate thickness were comparatively small so the average Charpy curve is shown.

It is evident that the Charpy test establishes the temperature range in which the dynamic toughness is increasing but the quantitative correlation of Charpy energy with dynamic toughness varies by a factor of 5 from steel to steel. At a dynamic toughness of 40 ksi$\sqrt{\text{in}}$. (44 MPa$\sqrt{\text{m}}$) steel G40.4 has a Charpy energy of 9 ft lb (12 J) and steel G40.11B has about 45 ft lb (61 J).

Another important observation is that there is, evidently, no thickness effect in the stress intensity for fracture initiation in the transition temperature range. This rather unexpected result may depend on the fact that all comparisons are being made in the temperature region where crystallographic cleavage is possible. There is a thickness effect but it shows up in the force level

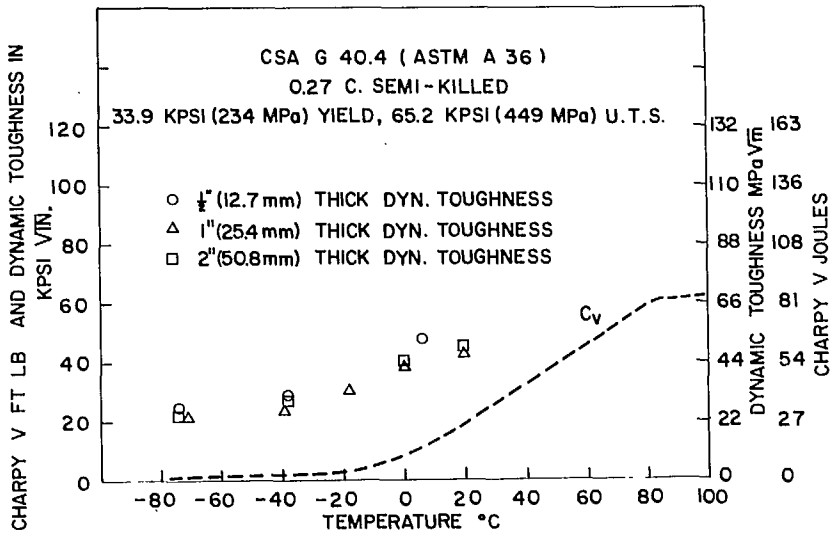

Fig. 5. CSA G40.4 (ASTM A 36) Steel. The 1-in. thick specimens are slightly below, and the 1/2-in. thick ones slightly above the 2-in. ones. This trend may result from chance or from differences in plate properties through the thickness.

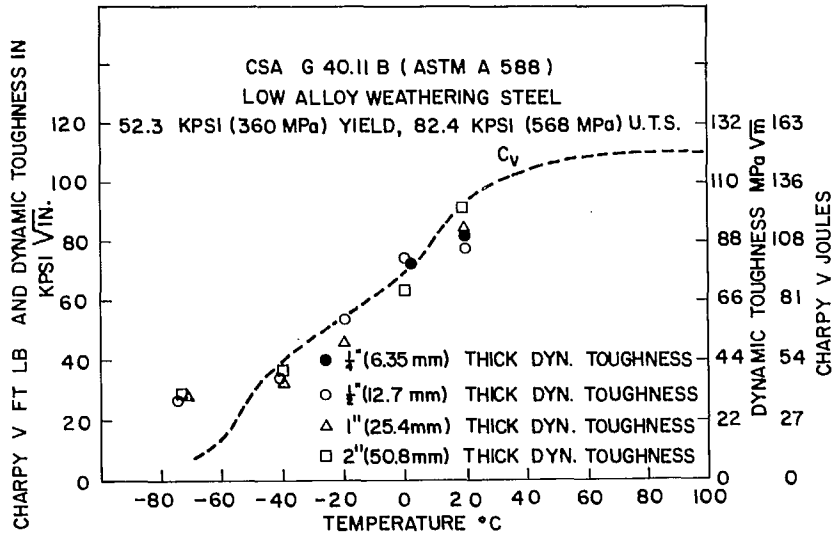

Fig. 6. CSA G40.11B (ASTM A 588) Steel. There is no consistent thickness effect on the stress intensity for fracture initiation.

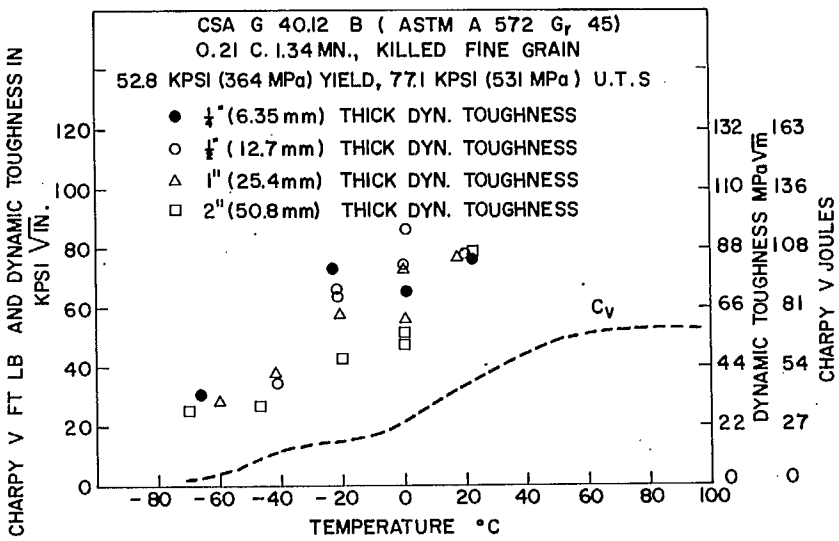

Fig. 7. CSA G40.12B (ASTM A 572) Steel. The scatter in test-results is unusually high in the middle of the transition range for thinner specimens machined from the 2-in. thick plate. There was some consistent inhomogeneity in Charpy energies through the plate thickness but it is not known whether inhomogeneity is the major cause of this scatter.

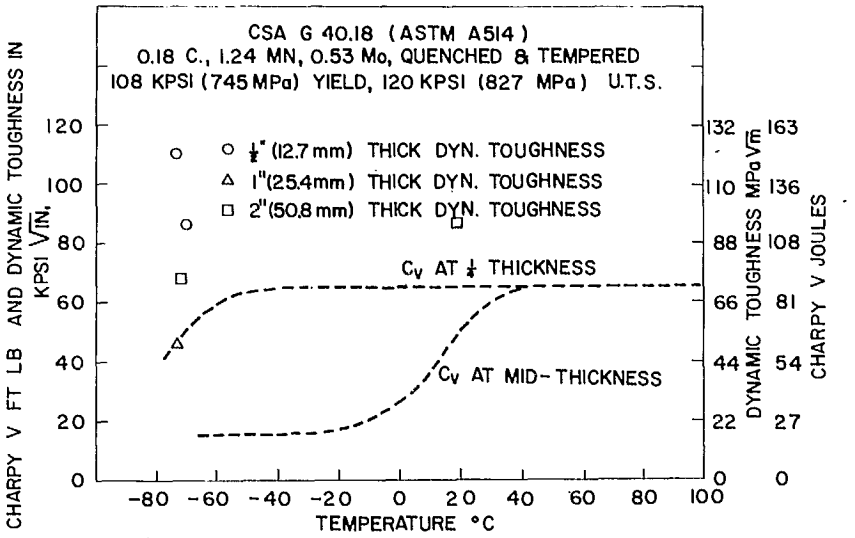

Fig. 8. CSA G40.18 (ASTM A 514) Steel. The properties at mid-thickness were poorer than near the surface but at -72°C the 2-in. thick plate still required a force of about 1/3 the peak value to propagate the fracture. The properties for thinner specimens depended on the thickness location from which they came so there was little point in an extensive series of tests. There was no load drop in the load-time trace for the 2-in. thick specimen at room temperature, so this data point is not quantitatively useful.

required to complete the fracture. This may be seen in Fig. 9 a, b and c for G40.12B steel at room temperature. While the initial peak stress and hence the stress intensity is constant, the load drop after the peak decreases and disappears as the thickness decreases. The fracture changes from a comparatively brittle type controlled by initiation to a ductile tear. Of course, if specific energy absorption was being measured a thickness effect would be found. A reason for the change in the force requirement to complete the fracture is that the percentage of oblique fracture increases as the thickness decreases.

Many of the stress intensities shown in the graphs are beyond the limits considered valid by ASTM Spec. E 399 and, in calculating these, reliance has been placed on the relationship

of stress intensity to crack tip strain mentioned in Section 2. This appears to hold for constrained flow but calculating the limits of constraint for these tests by the method in Reference 5 is complicated because, with large plastic zones, the relevant strain rate and, hence, yield strength becomes indefinite and, as well, the nominal stress is very high. For these reasons it seems preferable, at present, to approach higher toughness dynamic fracture characteristics primarily by experiment. If the stress-time curve for the fracture shows, as in Fig. 9a, a peak load attained in less than a millisecond followed by a sudden load drop and a comparatively low force to complete the fracture, then it is a "brittle" fracture. One can determine, experimentally, the stress-time characteristics for a specimen that simulates the structural geometry as closely as possible. Then the ductility level at which the fracture changes from the constrained type to the tear type can be determined for that application. At the higher ductility levels such applications would be those where load can follow deflection.

It might be of interest to note here some information on the effect of ductility at the empirical nil-ductility temperature obtained from a comparison of tension test and dynamic test results on the "calibration plate". The NDT temperature was about -18°C and there was an arrested "pop-in" at 39.6 ksi (272 MPa) at -35°C and a through fracture at 41.3 ksi (285 MPa) at -15°C. The arrested fracture at -35°C indicates that the dynamic "pop-in" toughness was less than 50 ksi$\sqrt{in}$. (55 MPa$\sqrt{m}$) and that the figure for a through fracture was higher than this amount. The dynamic stress-time curve at -20°C is shown in Fig. 10. It may be noted that considerable load remained as the fracture progressed. The maximum load gives a dynamic toughness of 33 ksi$\sqrt{in}$. (36 MPa$\sqrt{m}$). This indicates that, in the tension tests, the requirement for satisfying the displacement condition for propagation had a major influence on the failure strength.

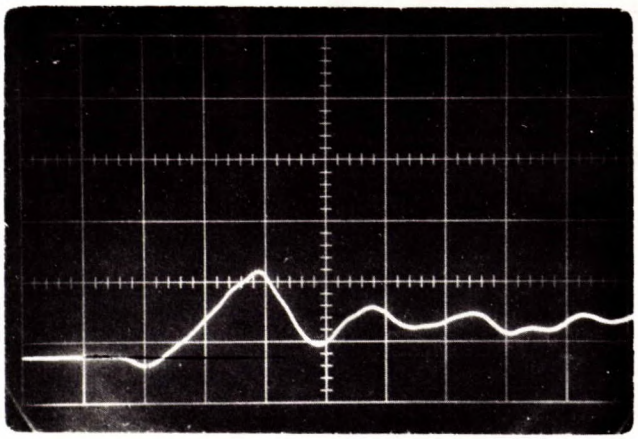

Fig. 9a G40.12B steel 2 in. (50.8 mm) thick at 22°C.

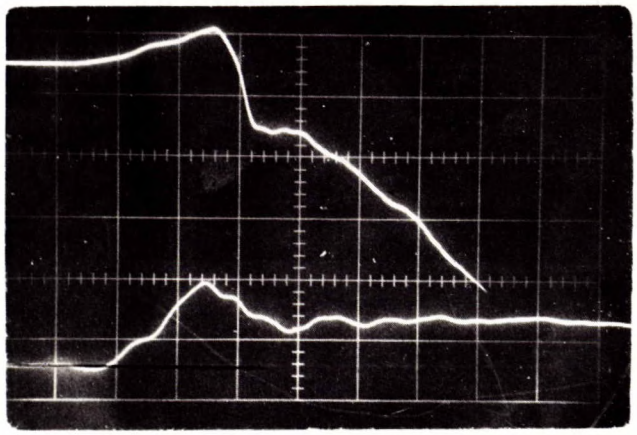

Fig. 9b. G40.12B steel 1 in. (25.4 mm) thick at 17°C. Disregard the upper trace.

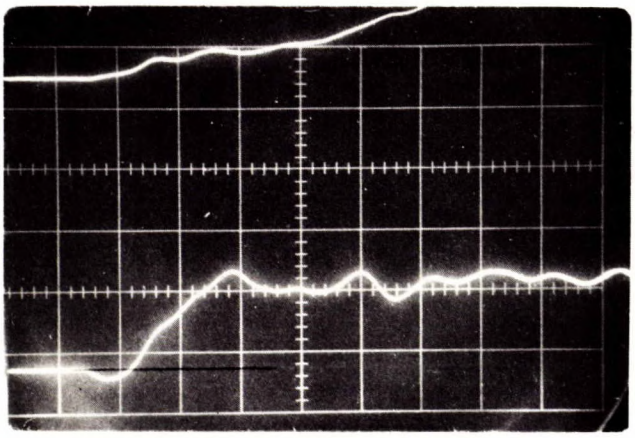

Fig. 9c. G40.12B steel 1/2 in. (12.7 mm) thick at 20°C. Disregard the upper trace.

Fig. 9. In all cases the horizontal scale is 0.2 millisec per division and the vertical is 500 microstrain per division. The initial load peak gives the same stress intensity in all three cases but the relative force required to complete the fracture increases as the thickness decreases. The fracture changes from a constrained type in 9a to a tear type in 9c.

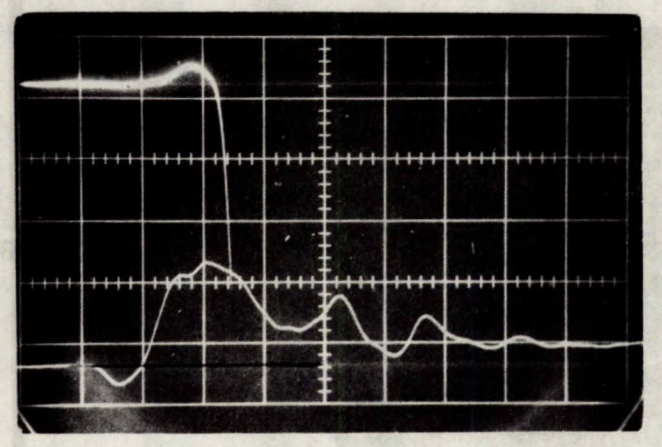

Fig. 10. "Calibration Plate" steel 3/4 in. (19 mm) thick tested at -20°C with the horizontal scale 0.2 millisec per division and the vertical 200 microstrain per division. Disregard the upper trace. The maximum load indicates K_{Id} = 33 ksi$\sqrt{in}$. (36 MPa$\sqrt{m}$). This test was done at the empirical drop-weight nil ductility temperature and it may be seen that considerable force was required, after the load peak, to complete the fracture.

ACKNOWLEDGEMENTS

Instrumentation was a vital part of this project and all of the instrumentation work was done by F.W. Marsh and K.A. Rocque. The fatigue pre-cracking of the specimens was done by J.A. Ellis.

LPT:gt

REFERENCES

1. L.P. Trudeau, "Radiation Effects on Toughness of Ferritic Steels for Reactor Vessels"; ASM-USAEC Monograph (Rowman and Littlefield, Inc., New York), pp 17-19, (1964).

2. L.P. Trudeau, "Mechanism of Low-Stress Brittle Fracture in Normally Ductile Materials"; Mines Branch Research Report R 190, Department of Energy, Mines and Resources, Ottawa, Canada, (Jan. 1967).

3. W.J. Hall, S.T. Rolfe, F.W. Barton and N.M. Newmark, "Brittle Fracture Propagation in Wide Steel Plates"; Final Report of Project SR-137 to Ship Structure Committee, National Academy of Sciences, National Research Council, Washington, D.C., (Oct. 1961).

4. O. Vosikovsky, "Strain Fields of Cracks under Tension Including Thickness Effects, Part 1. Experimental Results"; Int. J. Fracture, vol. 10, No. 2, pp 141-157, (June 1974).

5. L.P. Trudeau and O. Vosikovsky, "Strain Fields of Cracks under Tension Including Thickness Effects, Part II. Correlations", Int. J. Fracture, vol. 10, No. 2, pp 159-166, (June 1974).

6. A.K. Shoemaker and S.T. Rolfe, "The Static and Dynamic Low-Temperature Crack Toughness Performance of Seven Structural Steels"; Eng. Fracture Mech., vol. 2, No. 4, pp 319-339, (June 1971).